Microscopic Structures in Turbulent Diffusion Flames*

Tamio IDA** and Kazutomo OHTAKE***

Microscopic structures in turbulent diffusion flames are studied by time-resolved temperature distributions measured by a laser-sheet-illuminated Rayleigh scattering (LRS) method recorded by a high-speed VTR system, and one-point LRS measurement. The microscopic structures of temperature distribution are measured by analyzing the two-dimensional LRS pictures by image processing. Coaxial turbulent diffusion flames at moderate Reynolds numbers, which exhibit typical diffusion flame structures, are formed on laboratory-scale burners. It is found that the flame can be divided into four characteristic regions based on the distributions of macroscale temperature fluctuations. These four regions are visualized by the two-dimensional LRS images. The turbulent heat-transfer mechanisms in these four regions are discussed in terms of the two-dimensional LRS and the power spectral density of temperature fluctuations measured by one-point LRS. Clusters of temperature inhomogeneity are observed by the image analyses in Regions I and III. It is found that different structures of microscopic temperature inhomogeneity exist within Taylor's dissipation length scale defined by velocity fluctuations.

Key Words: Diffusion Combustion, Combustion Phenomena, Spectroscopic Measurement, Texture Analysis, Two-Dimensional Laser Rayleigh Spectroscopy, Microscopic Inhomogeneity of Flame Structure

1. Introduction

Space- and time-resolved fundamental information, such as velocity, temperature and concentrations of chemical species, is quite essential for the detailed study of mixing, reaction and heat-transfer mechanisms in a turbulent diffusion flame. In the authors' previous studies, the turbulent diffusion flame structures were studied by time-resolved one-point LRS measurement. The turbulent time scale was obtained therein from the temperature fluctuations. It was determined that the flame could be divided into four regions based on the characteristics of time scale. The time-dependent phenomena have often been masked by the statistical analyses, and the spatial structures of turbulent diffusion flames are not yet fully understood.

* Received 27th November, 1992. Paper No. 91-1643

** Department of Mechanical Engineering, Kumano Technical College, 2800 Arima-cho, Kumano, Mie 519-43, Japan

*** Department of Ecological Engineering, Toyohashi University of Technology, 1-1 Tempaku-cho, Toyohashi, Aichi 441, Japan

Recently, new laser spectroscopy techniques have been adopted to measure the planar images of scalar quantities in the reacting flows by using a laser sheet as an incident light source[1]-[9]. Such spatial information cannot yet explain the heat-transfer mechanisms occurring in the mixing process without additional information. Various methods such as fluorescence and Mie scattering have been used to measure the species concentrations and instantaneous shapes of flame and/or fuel flow. With planar fluorescence spectroscopy it is slightly difficult to obtain qualitative information for the entire observation area since it is rather hard to excite all of the target molecules in the saturated condition[10]. On the other hand the Mie scattering method is the easiest technique for obtaining the plane images[1]-[3]. However, the difficulty in uniform introduction of fine particles into the flow remains a problem. An LRS can measure the time-resolved gas temperature in the reaction flow if the bulk scattering cross sections of the air, fuel and combustion gas mixture does not change very much before, during and after the combustion.

Fourguette et al.[4] presented a time-resolved two-dimensional LRS to map the instantaneous

temperature of a non-premixed flame. They obtained important information for the large-scale structures in the turbulent mixing region between fuel flow and surrounding air. On the other hand, Gouldin[1] and Takeno and Murayama[2] attempted to predict the turbulent burning velocity and discuss the flame structures in premixed turbulent flames by fractal analyses applied to the images obtained by laser tomography. Some papers correlated the recorded signals of the phenomena occurring in the flame with the images taken simultaneously.

This study discusses in detail the microscopic structures of temperature inhomogeneity existing in the focused point, which corresponds to a minute volume, of incident laser light to measure the one-point local temperature by LRS thermometry. Typical microscopic structures were found to correspond to the mixing and reacting mechanisms in each region. Texture analyses were carried out to clarify the spatial and time-resolved mechanisms of turbulent combustion in the tested flames. The microscopic clusters of temperature inhomogeneity were found to exist within Taylor's dissipation length.

2. Experimental Apparatus

Figure 1 shows the alignment of the optical system. The LRS at the wavelength of 488 nm supplied from an Ar ion laser was adopted to measure the flame temperature. A pair of spherical multireflection mirrors reflected the laser light about ten times to intensify the incident light power at the focused point. This system could detect the temperature fluctuation up to 10 kHz for one-point measurement. In order to measure the two-dimensional microscopic structure of temperature fluctuations in the focused point, the combination of a close-up lens and bellows system enlarged the local temperature distribution inside the area of 0.22×0.44 mm^2. The image intensifier was used to strengthen the power of the image of scattered light. A high-speed video camera (nac 400) recorded the thus-enlarged and intensified LRS images. The area of one pixel was calibrated as 1.79×1.79 μm^2 by taking an image of a standard mesh.

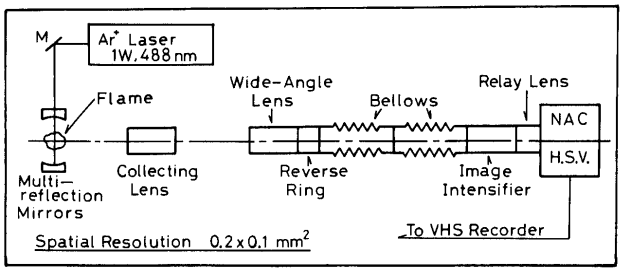

Fig. 1 Alignment of optical system

The mixed gaseous fuel of 62.2% H_2+37.8% CH_4 was fed to the coaxial burner in which a fuel pipe of 2 mm I.D. was surrounded coaxially by an air pipe of 64 mm I.D. Burner Reynolds number was fixed at 5 000. The bulk Rayleigh scattering cross section of this fuel does not differ by more than 5% from those of air, fuel and burnt gas before, during and after combustion. The test section was fixed at $x/D=25$.

A pair of LDV systems was adopted to measure Taylor's dissipation length by two-point correlation of velocity fluctuations at 50 and 51.15 mm above the burner tip, respectively. Talcum powder of 2 μm nominal diameter was used as the seeding particle for LDV measurement.

3. Image Analysis

The time-resolved VHS image was converted into an RGB plane of 511×511 pixels. The LRS signal stored in the region of 125×250 pixels in the G-image plane was selected to be converted into the temperature signal. The irregularity of incident laser intensity in the measuring plane was corrected before conversion by the intensity pattern obtained at 300 K. Flame luminosity always varies in the signal in Regions I and II ; we must correct this effect. However, attention must be paid to the signal in Region III since there exist moments when the flame zone covers the entire area, and the air forms the large-scale roll-up eddies which entrain the surrounding air into the flame region. Figure 2 shows the probability density functions (PDF) of typical LRS signals in the cases where the flame region exists within the frame, for PDF of background at 300 K and where flame luminosity appeared in the converted G-plane. The PDF of flame luminosity was almost constant for all these cases, and it was corrected before conversion. The lower limit of the time difference for the correspondence between the LDV signals at two measuring points was determined as 1.6 kHz to obtain the velocity correlation. This value was selected as the aerodynamic

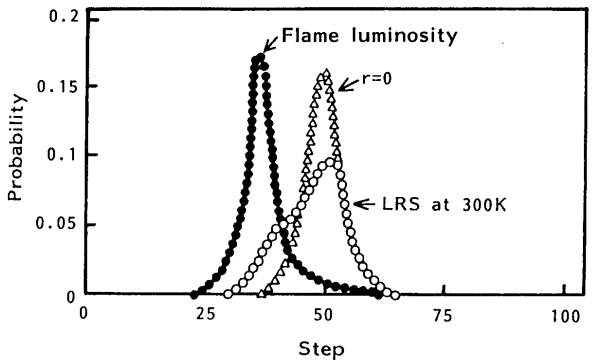

Fig. 2 Probability distributions of quantities included in raw data

following-up ability of seeded fine particles to the gas flow and was estimated as 5 kHz; the data pairs within an internal three times as long this characteristics time interval were used in the analysis.

4. Results and Discussion

The results obtained by cluster analysis, with different sizes of spatial filters, of the instantaneous two-dimensional LRS signals are discussed and the spatially averaged temperature in the measured area and that obtained by the one-point measuring method are compared.

4.1 Instantaneous two-dimensional temperature distribution

Figure 3 shows the instantaneous temperature distributions in the measured area with spatially by averaged temperature $[\overline{T}]_s$ at radial position r from the center line in the plane of $x/D=25$ at $Re=5\,000$. These results can explain the characteristics of turbulent diffusion flame structures in the four regions discussed in the previous paper as follows[11)-13)]. Region I corresponds to that of the fuel jet, and small areas of higher temperature are observed in lower and weakly fluctuating temperature fields. Region II is located between Regions I and III, and here the combustion takes place between the fuel and air, entrained from Region III, mixed by the turbulent motions. The measured area is almost always covered by the fluctuating high-temperature signals and high spatially averaged temperature results for almost all the frames. Region III entrains the surrounding air by large eddy motion and the typical entrainment behaviors appear between the fuel and air. There are instances at which cold air and fuel cover the measured area and high-temperature combustion gas exists under a homogeneous, coherent and weak turbulent condition. Similar behaviors as those in Region I are observed in this region. Region IV corresponds to the surrounding air flow and shows low and constant temperature distributions, however, occasionally gas at moderate temperatures diffuse into this region from Region III, and islands of cooled combustion gas are formed.

Figure 4 shows the time-resolved spatially

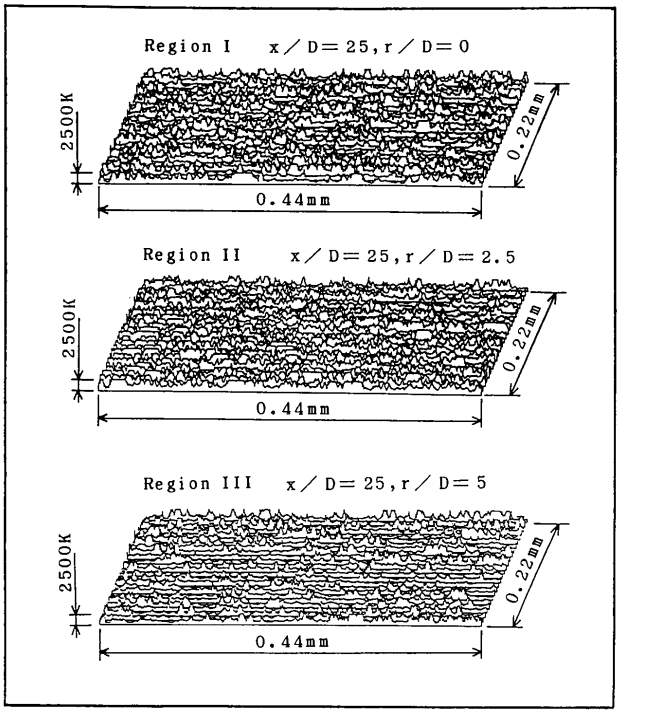

Fig. 3 Instantaneous temperature distributions in the measured area [0.22×0.44 mm²]

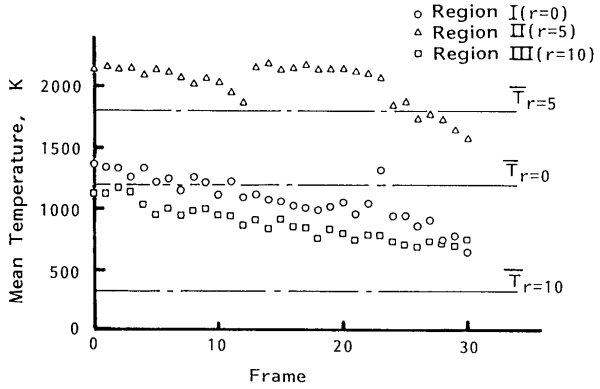

(a) Time history of spatially averaged temperature

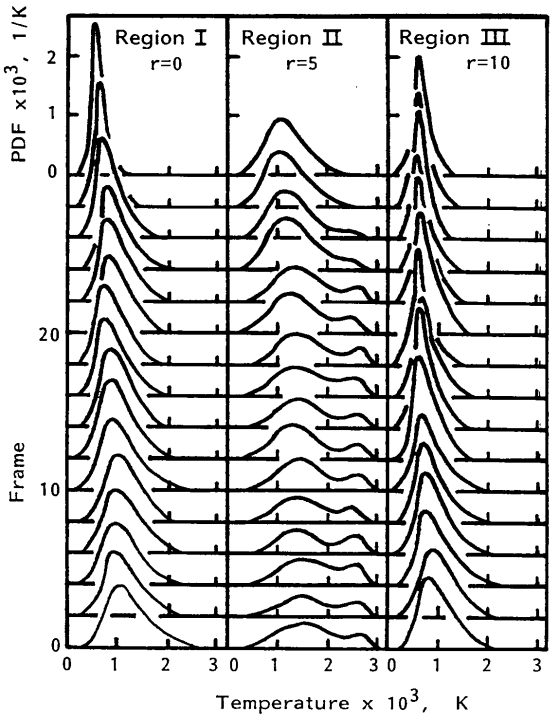

(b) Time history of probability density function

Fig. 4 Time history of spatially averaged temperature and probability density functions in three regions

averaged temperature and PDF of temperature inside the measured area for thirty successive frames. Time mean temperature by one-point measurement is also shown for comparison. The difference between spatially averaged temperature and time mean temperature is not very marked in Region I and II. On the other hand, in Region III the spatially averaged temperature is from 300 to 800 K higher than the time mean temperature. One of the reasons for this difference might be considered as the influence of the flame luminosity, but the main reason is the fact that the series of frames containing high-temperature clusters have been selected.

The time histories of PDF in Regions I and III show that they cover a wider ranges of temperature, have shapes close to the Gaussian distribution and do not change markedly. In Region II PDF cover wide temperature range than in the other two regions, and is shaped bimodal distributions. These are in line with the results reported by Fourguette et al.[4] with their visualization experiment by the LRS method. This study clarifies that this kind of bimodal characteristic exists within the microscopic flame structures. In order to examine the flame structure in more detail, the results will be compared with those obtained by one-point measurement.

4.2 Comparison between instantaneous temperature distribution by two-dimensional measurement and time-sequential temperature by one-point measurement

Figure 5 compares PDF obtained from the typical instantaneous two-dimensional temperature distribution with that from the 10 000 data points of one-point measurement (these data points correspond to those during 0.17 s.). In Region I, PDF from one-point measurement shows Gaussian distribution near the middle of PDF from two-dimensional measurement. In Region II the former appears in a near-Gaussian distribution at the valley of bimodal distribution of the two-dimensional measurement.

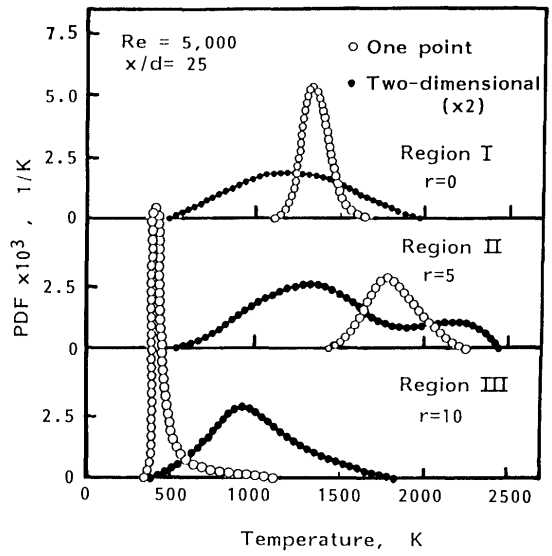

Fig. 5 Comparison of PDF between the instantaneous two-dimensional and one-point temperature measurement

From these results, it is found that Region I consists of microscopic inhomogeneous spatial temperature distribution which are formed by small islands of combustion gas separated from the flame region flowing into the cooler fuel flow and/or the separated small air chips flowing into the cooler fuel flow, and small combustion gas islands might be distributed. However, one-point measurement only produces the spatially averaged temperature by integrating the entire distribution over in the volume, hence it could not detect this microstructure; it produces the time sequential temperature history shown in Fig. 4. Region II is the combustion region and produces the microscopic inhomogeneity by the interactions between aerodynamic turbulence and chemical reactions.

4.3 Cluster analysis by spatial filter

A slight difference could be observed in the characteristic structures of Regions I and III from the spatial temperature distributions shown in Fig. 3. Cluster analysis was applied to the converted images to make their differences clearer. Different sizes of spatial filters with the same weight to every pixel were used to enhance the inhomogeneities in the images. Temperature was divided into two categories, one higher than 1 500 K which is dark, the other lower than 1 500 K shown by blank spaces. Typical examples for Regions I and III are shown in Fig. 6 in which the clusters become clearer with the larger-sized spatial filters. The cluster distributions do not change very much when the filter size becomes larger than 7×7. The difference between Regions I and III becomes clearer after this cluster analysis. In particular, in Region III the effect of filtering in cluster analysis begins to appear with the use of a relatively small 3×3 filter, and becomes marked at the filter size of 5×5. The results for Region II are almost completely dark, which shows the field is occupied by burnt gas and/or a burning zone; it is not shown here.

In order to discuss the above-mentioned microscopic flame structures, the one-dimensional power spectral density for each region is shown in Fig. 7. In Region I the turbulent thermal diffusion effect shown by the $-5/3$ power law is observed up to the higher-frequency region. This corresponds well to the fact that the microscopic high-temperature clusters diffuse into the fuel flow region due to the aerodynamic

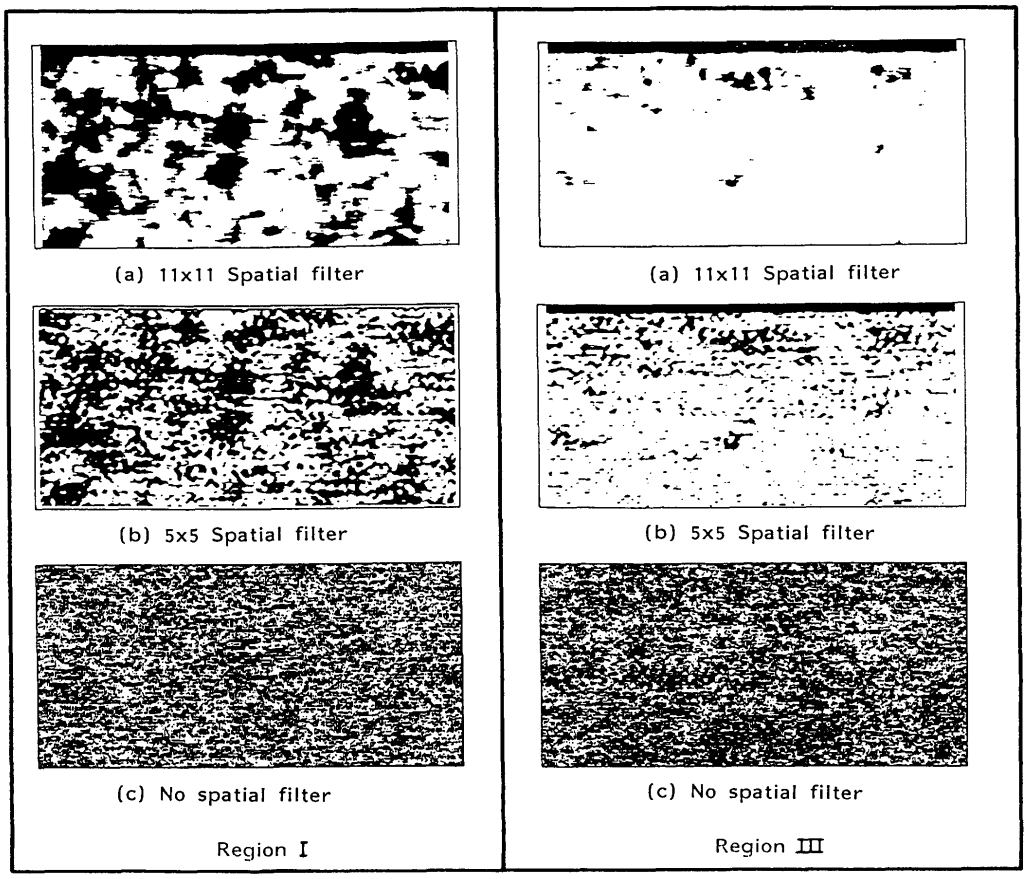

Fig. 6 The effect of spatial filter sizes on cluster analyses

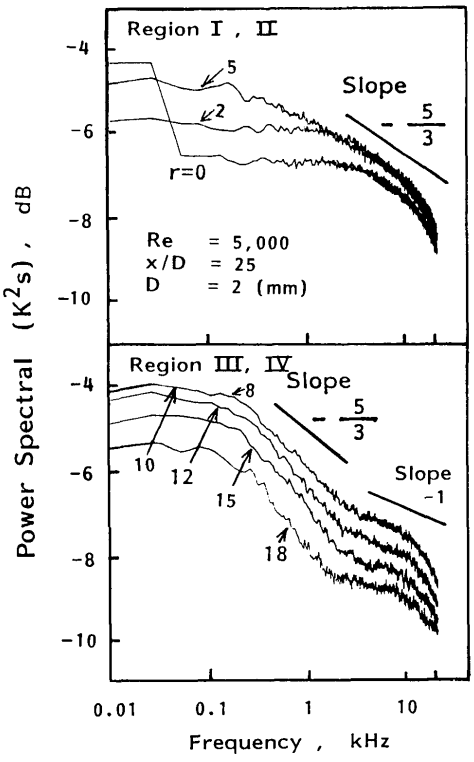

Fig. 7 One-dimensional power spectral density for each region calculated by one-point measurement

turbulent motions, as shown in Fig. 6. Contrary to this, in Region III the $-5/3$ power law region is observed at lower frequency. This is well understood from the Schlieren photography and two-dimensional laser tomography taken by the high-speed VTR system and presented in the previous paper[9] that this power law corresponds to the aerodynamic mixing due to rather large structures, and the finer cluster may indicate the -1 power law, showing the diffusion due to molecular-level mixing which exists at the regions of mild temperature gradient at the moderate-temperature range. As mentioned above, in Region II marked clustering could not be observed using the 3×3 spatial filter, but the clusters existing within the temperature range above 1 500 K might be aerodynamically diffused due to the turbulent mixing. The bulk gas flow speeds in Regions I and II are so high that the electric circuit could not record the density in the frequency region in which the -1 power law is observed. In Regions III and IV this could be recorded since the flow speed is lower than those in Regions I and II.

In order to observe the time history of variations of clusters the typical time sequence results in Regions I and III obtained with the 11×11 spatial filter are shown in Fig. 8. As seen in the results for Region I,

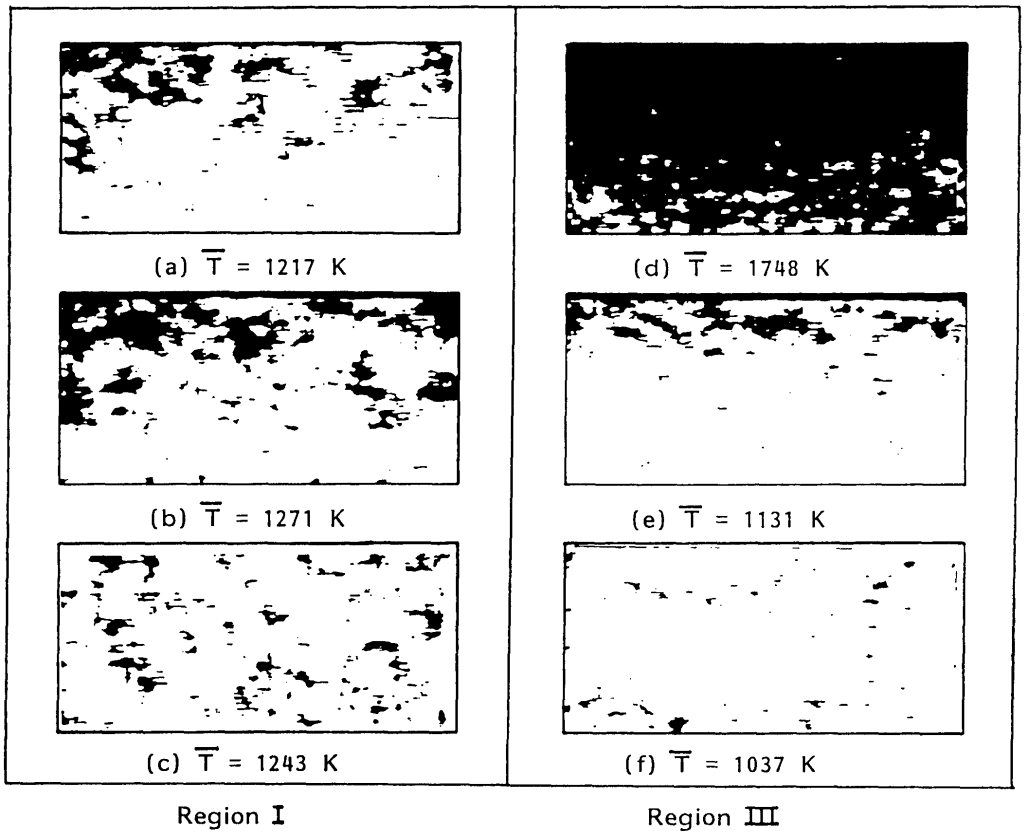

Fig. 8 Typical time sequence results of cluster analyses in Regions I and III by the 11×11 spatial filter

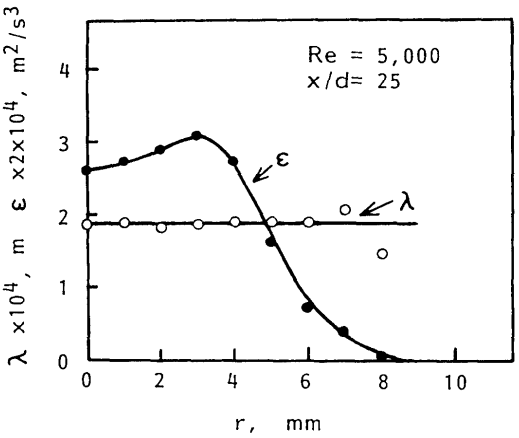

Fig. 9 The distributions of Taylor's dissipation length λ and dissipation rate of kinetic energy ε based on the data obtained using an LDV

the sizes of high-temperature clusters flowing from Region II are similar and distributed evenly within the area, and this may give the result of weak variation of temperature signals in one-point measurement. The changes of cluster sizes and their distributions in Region III are caused by the large-scale eddy motions of the surrounding air entrained from Region IV. Therefore, the patterns of cluster distributions change drastically from the range of flame regions to the air flow. The values of time mean temperature show the spatially averaged temperature over this two-dimensional area.

The above discussions show that the degrees of spatial connection or the distributions of temperature gradient which directly affect the turbulent diffusion flux greatly affect the determination of turbulent diffusion flame structures.

4.4 Examination of validity for inhomogeneity

As the reference of scales for temperature clusters, Taylor's dissipation length (λ)[14] defined by Eq. (1) was calculated base on the experimental data obtained by the cross-correlation between the velocity fluctuations obtained by pairs of data at two different points using the LDV method.

$$\lambda=\left[\overline{u'^2}\Big/\overline{\left(\frac{\partial u'}{\partial x}\right)^2}\right]^{1/2} \qquad (1)$$

The results are shown in Fig. 9 for the dissipation rate of kinetic energy ε as a function of radial distance r. It is clear that λ was almost constant over the radial distance while ε varied greatly. The scales of inhomogeneity of temperature shown in Fig. 8 range from 40 to 200 μm. Considering that the value of λ gives the order of magnitude of the momentum of eddies, the scale of temperature inhomogeneities can be considered as almost equal to or slightly smaller

than that of λ. This shows that temperature clustering begins to be observed around the scale on the order of differential characteristic distance, and the scale of temperature clustering corresponds to the sizes at which the clusters begin to be affected by the molecular viscosity. Here we can summarize that this study quantitatively measured the characteristic sizes of mixing phenomena of reactants changing from turbulent to molecular-scale diffusion.

5. Conclusions

The following conclusions are derived for the spatial turbulent diffusion flame structures by various texture analyses appling the two-dimensional LRS method and comparisons with the conventional one-point measurement.

1) A method for measuring instantaneous two-dimensional temperature distribution has been developed. Texture analyses corresponding to the four regions characterized by the tendencies of time scales of turbulence in the previous paper have been carried out. The existence of the clusters of combustion gas flowing into the fuel flow was clarified.

2) The variations in the characteristics of spatial temperature gradients could be observed by changing the size of spatial filters for the converted images. The results indicated that the spatial distributions and their relationships to temperature gradients are very important in explaining the various thermal diffusion effects in the turbulent diffusion flames.

3) The existence of microscopic inhomogeneities of temperature was examined using Taylor's dissipation length, the statistical quantity of velocity field. It was shown that the sizes of temperature inhomogeneities were around or order of this dissipation length.

Acknowledgement

The authors would like to express their gratitude for partial funding through a Research Grand-in-Aid for Scientific Research on Priority Areas "Exploration of Combustion Mechanism" from the Ministry of Education, Science and Culture under Contract Number 02209102.

References

(1) Gouldin, F.C., Combust. Flame, Vol. 68, No. 3 (1987), p. 249.
(2) Takeno, T. and Murayama, M., Proc. 22nd Symp. (Int.) on Combust., (1988), p. 511.
(3) Gutmark, E., Hanson-Parr, D.M. and Schadow, K. C., Fractal Behavior of a Wrinkled Annular Diffusion Flame, Combust. Flame, Vol. 79 (1990), p. 7.
(4) Fourguette, D.C., Zurn, R.M. and Long, M.B., Two-Dimensional Rayleigh Thermometry in a Turbulent Nonpremixed Methane-Hydrogen Flame, Combust. Sci. and Tech., Vol. 44 (1986), p. 307.
(5) Miyawaki, K., et al., Proc. of 26th Combust. Symp. in Japan (1988), p. 22.
(6) Hanson, R.K., Combustion Diagnostics: Planar Imaging Techniques, 21th Symp. (Int.) on Combust., (1986), p. 1677.
(7) Mansour, M.S. and Bilger, R.W., Spatial-Averaging Effects in Raman/Rayleigh Measurements in a Turbulent Flame, Combust. and Flame, Vol. 82 (1990), p. 411.
(8) Namazian, M. and Kelly, J.T., Near-Field Instantaneous Flame and Fuel Concentration Structures, 22nd Symp.(Int.) on Combust., (1988), p. 627.
(9) Ohtake, K., Naruse, I., Horiuchi, K. and Tsuji, H., Structure of Turbulent Diffusion Flame by High-Speed Image Processing and Rayleigh Scattering, Trans. Jpn. Soc. Mech. Eng., (in Japanese), Vol. 57, No. 535, B(1991), p. 1135.
(10) Deguchi, Y., Yoshikawa, N. and Ohtake, K., Temperature and Concentration Measurement of OH by Three-Line Laser-Induced Fluorescence, Proc. 5th Int. Symp. Applicat. Laser Tech. Fluid Mech., (1990), p. 2.3.
(11) Ida, T., Horiuchi, K. and Ohtake, K., Turbulent Diffusion Flame Structures and Their Similarities, Joint Int. Conference Australia/New Zealand and Japanese Sections, (1989), p. 48.
(12) Ida, T. and Ohtake, K., Experimental Study of Diffusion Flame Structures and Their Similarities, Trans. Jpn. Soc. Mech. Eng., (in Japanese), Vol. 56, No. 531, B(1990), p. 3514.
(13) Ohtake, K. and Ida, T., Proc. 5th Int. Symp. Applicat. Laser Tech. Fluid Mech., (1990), p. 31.2.
(14) Townsend, A.A., The Structure of Turbulent Shear Flow, 2nd ed.(1980), p. 47, University of Cambridge.